η′ photo-production off nucleons

—Some evidence of $D_{15}(2080)$ in the reaction

Xian-Hui Zhong
Hunan Normal University

In collaboration with Qiang Zhao

Why we study η′ photo-production?

- The threshold energy of the η′ photo-production is above the second resonance region, which might be a good place to extract information of the less explored higher nucleon resonances around 2.0 GeV. Thus, the study of η′ photo-production becomes an interest topic in both experiment and theory.

I. Recent progress in η' photo-production : Experiments

CLAS Results

γp→η’p

PRL 96, 062001 (2006)

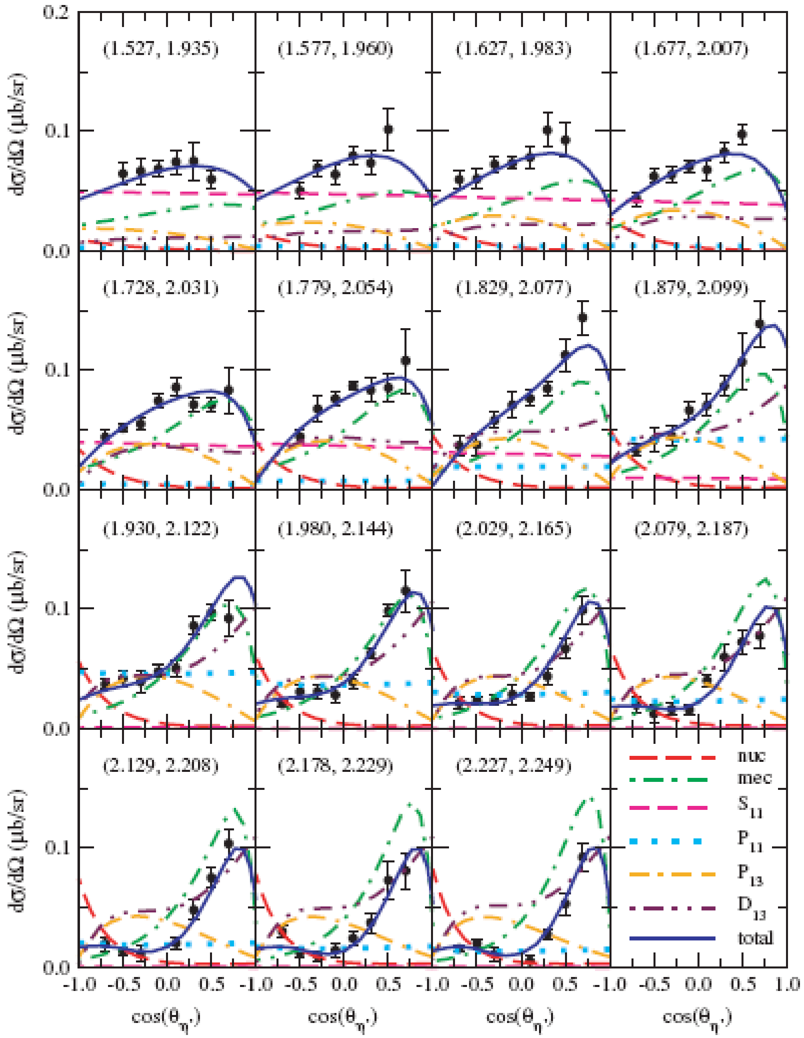

K. Nakayama et al, PR C 73, 045211 (2006)

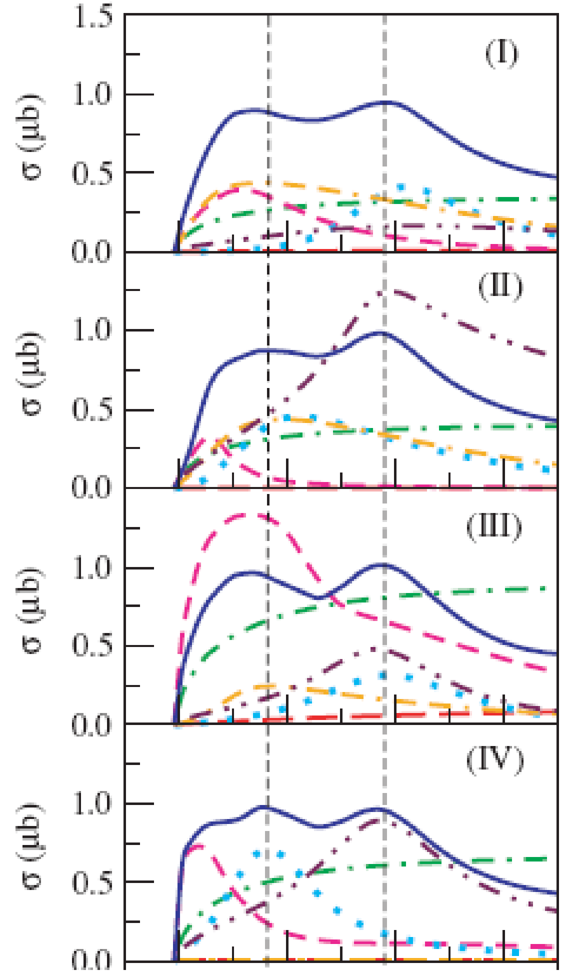

K. Nakayama et al analyzed the data, they predicted a bump structure in the total cross section at 2.09 GeV . If this is confirmed, the D_{13}(2080) and/ or P_{11}(2100) resonance may be responsible for this bump.

PR C 73, 045211 (2006)

CLAS Results

PR C 80, 045213 (2009)

$\gamma p \rightarrow \eta' p$

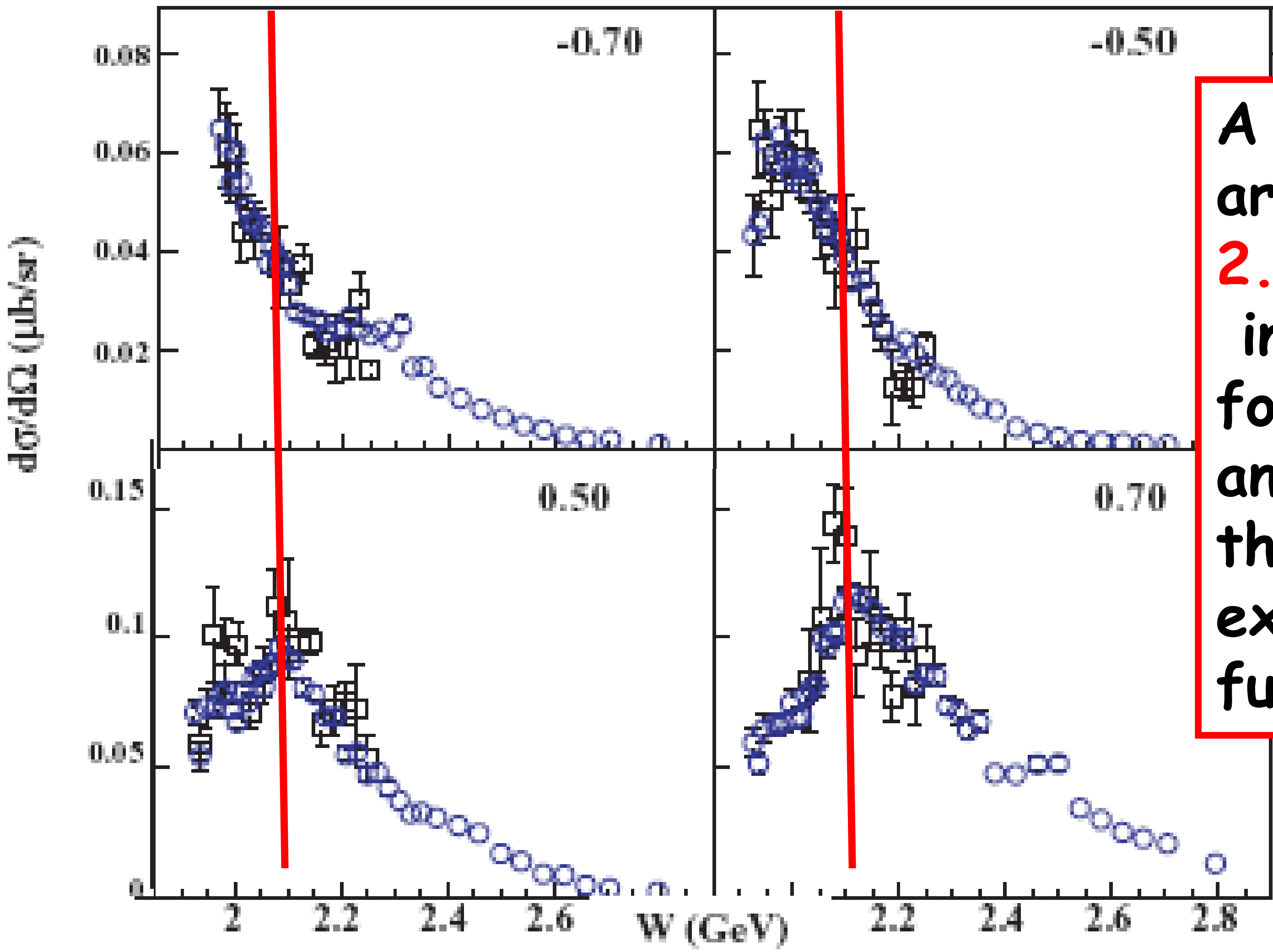

A bump around **2.1GeV** in the forward angle of the exciting function.

CLAS Results

$\gamma p \rightarrow \eta' p$

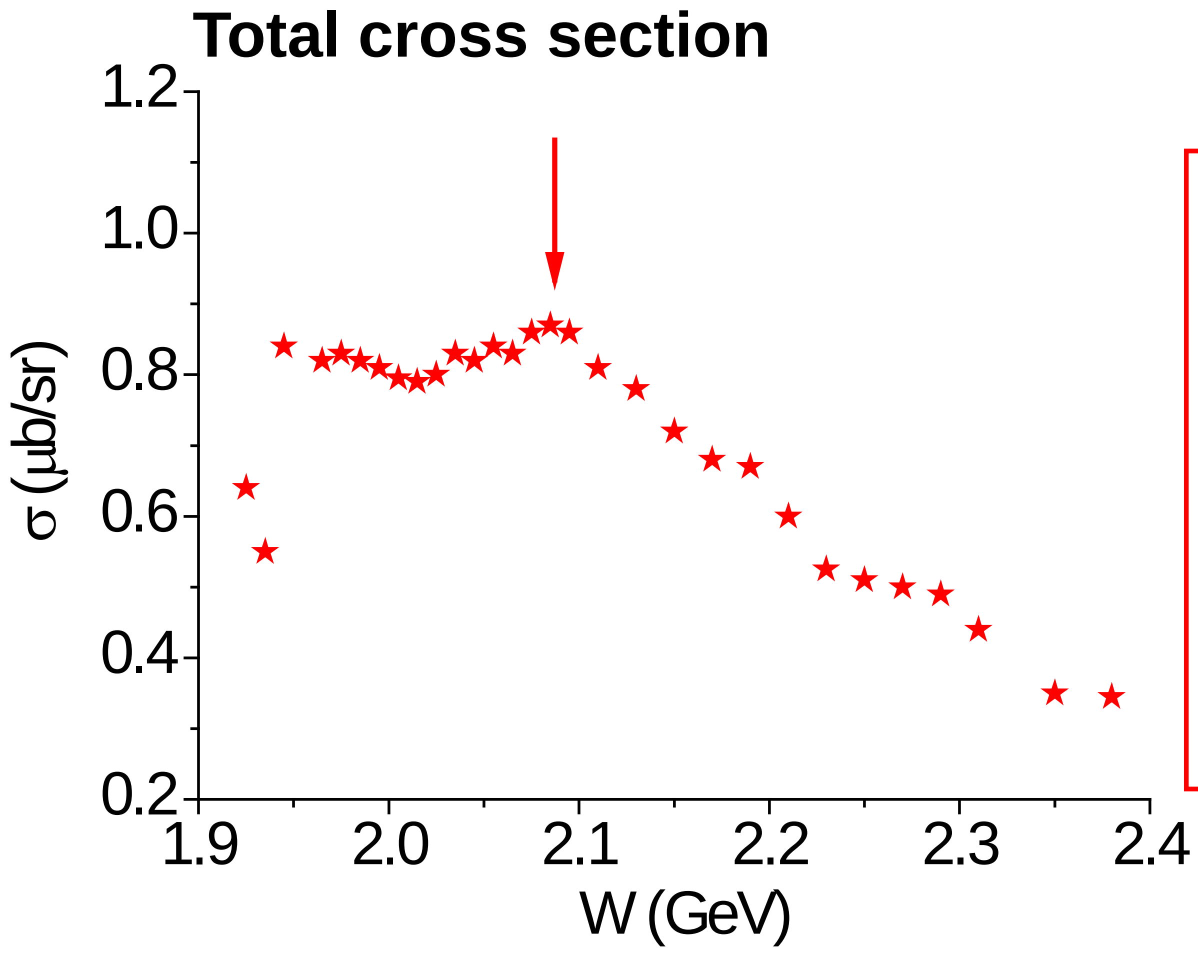

A bump around **2.1GeV** in the cross section.

PR C 80, 045213 (2009)

Differential cross sections

CLAS Results

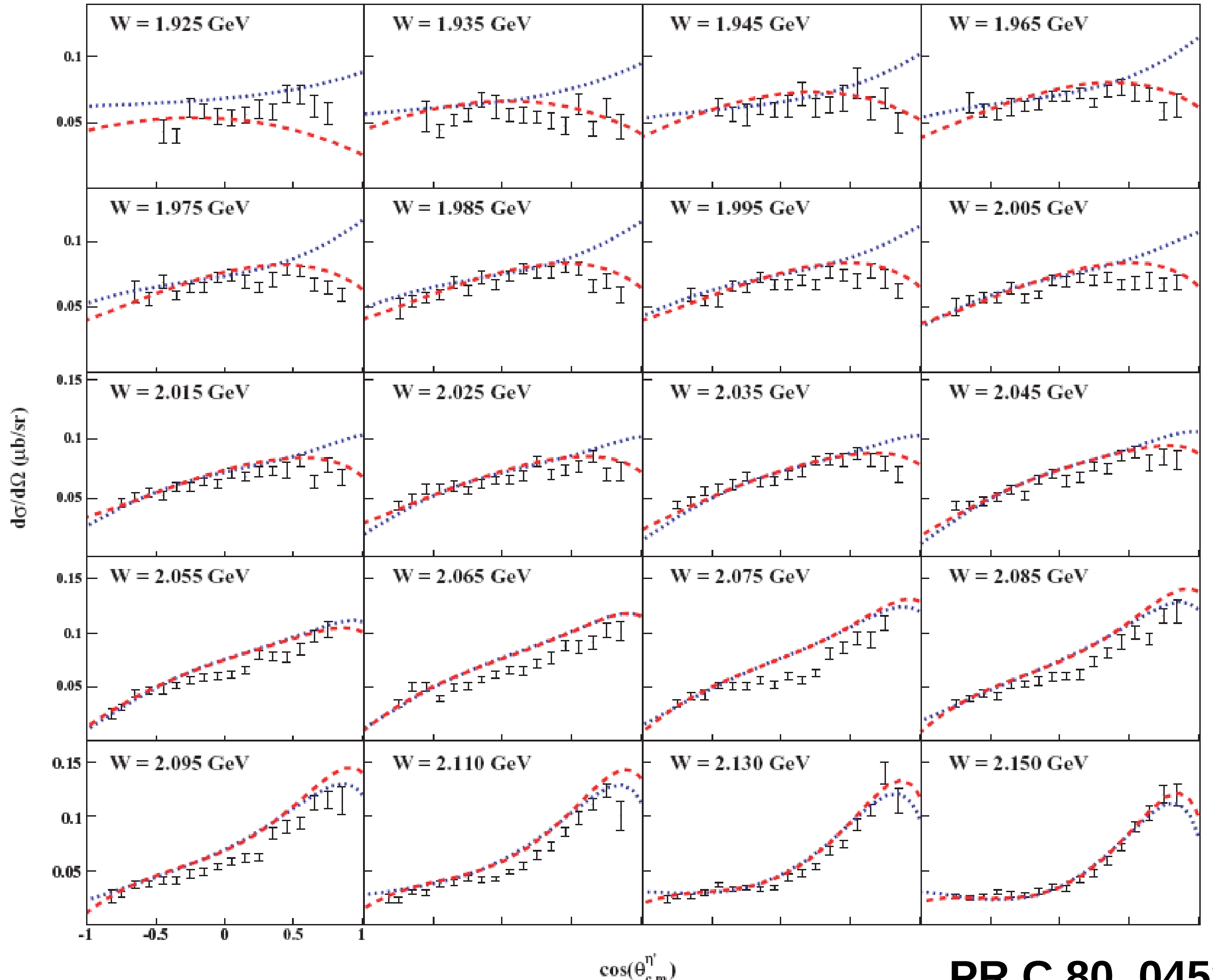

PR C 80, 045213 (2009)

FIG. 7. (Color online) $\frac{d\sigma}{d\Omega}(\mu b/sr)$ versus $\cos\theta^{\eta'}_{c.m.}$ for the $\gamma p \to p\eta'$ reaction. Note that the vertical axis is linear. The (red) dashed line and (blue) dotted line are the results from Tables II and IV of Ref. [16], respectively.

CBELSA/TAPS Results

γp→η'p

PR C 80, 055202 (2009)

Total cross section

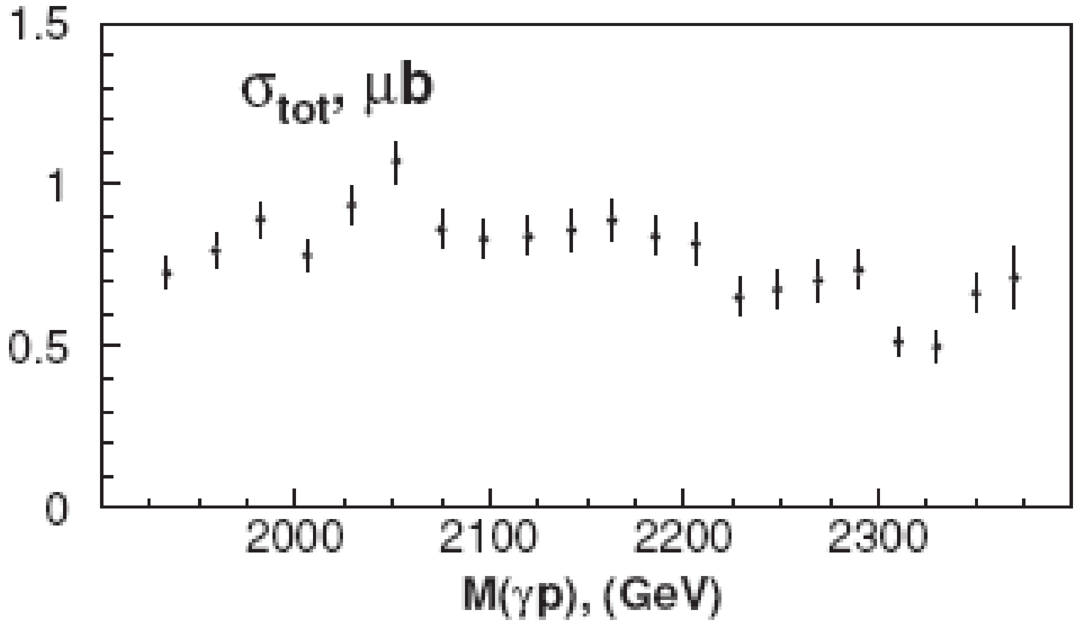

FIG. 15. Total $\gamma p \rightarrow p\eta'$ cross section. The data points (●) are calculated by summation of the differential cross section.

No obvious structure around 2.1GeV in the cross section.

CBELSA/TAPS Results

Differential cross sections

PR C 80, 055202 (2009)

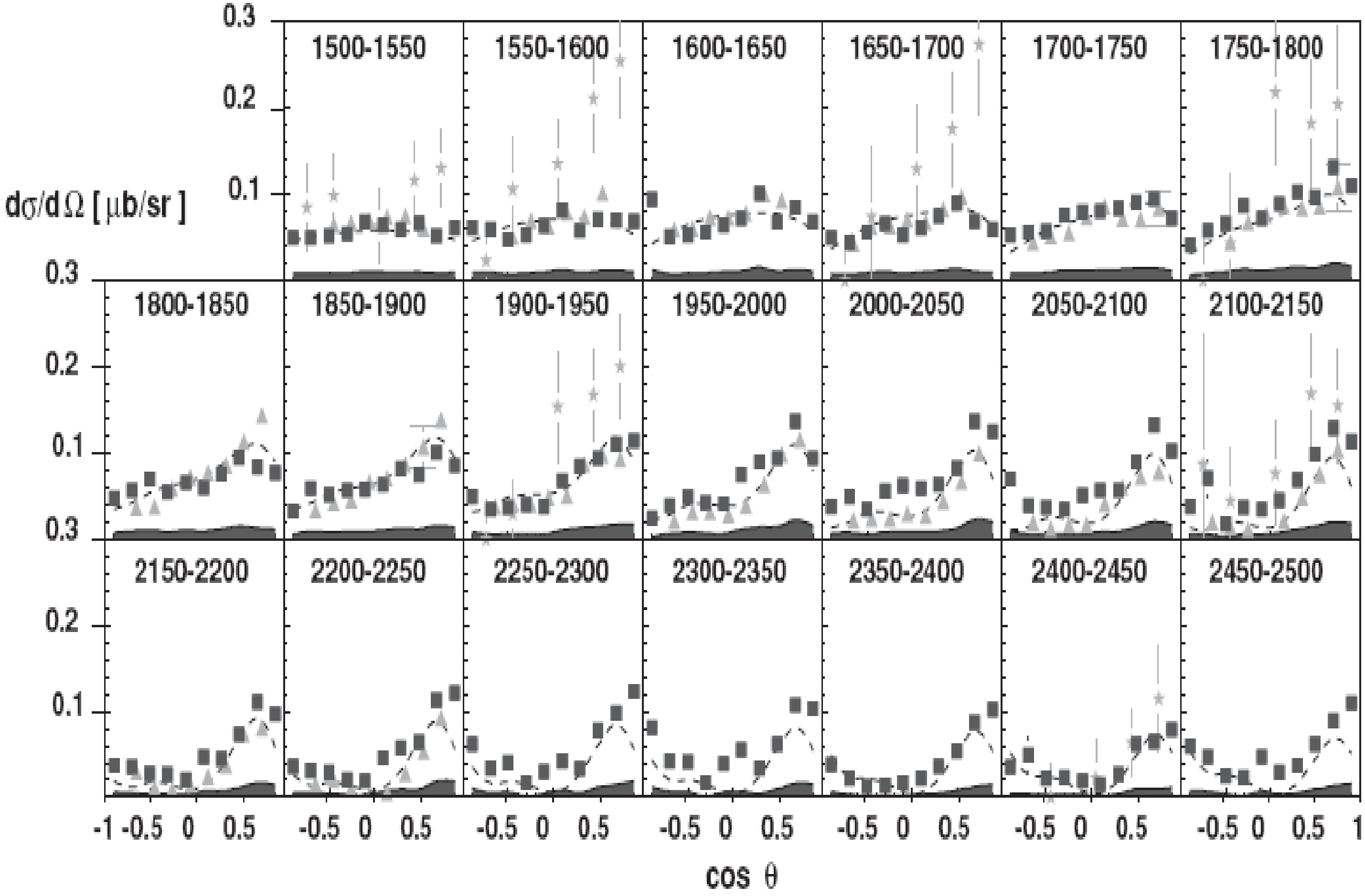

CBELSA/TAPS Results

Photoproduction of eta’ meson off the deuteron

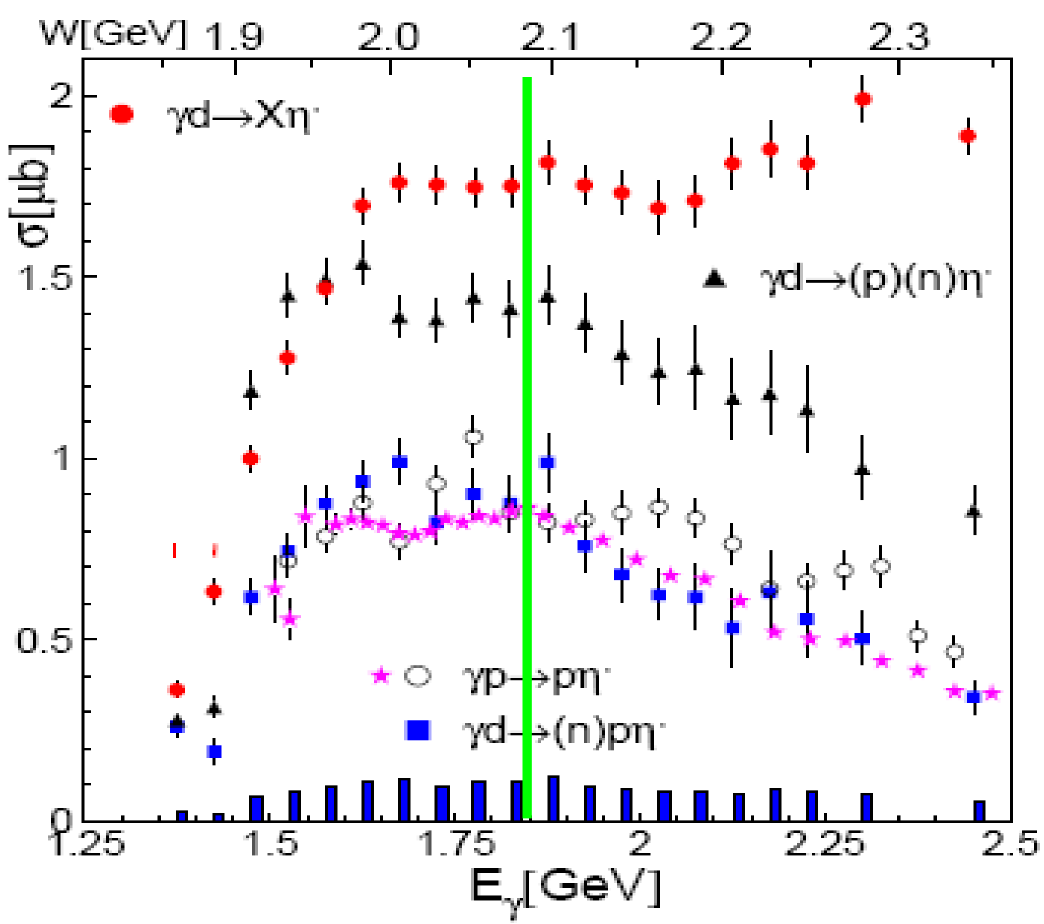

Eur.Phys.J. A47 (2011) 11

A bump-like structure appears around 2.1 GeV in the cross section.

CBELSA/TAPS Results

$\gamma p \rightarrow \eta' p$

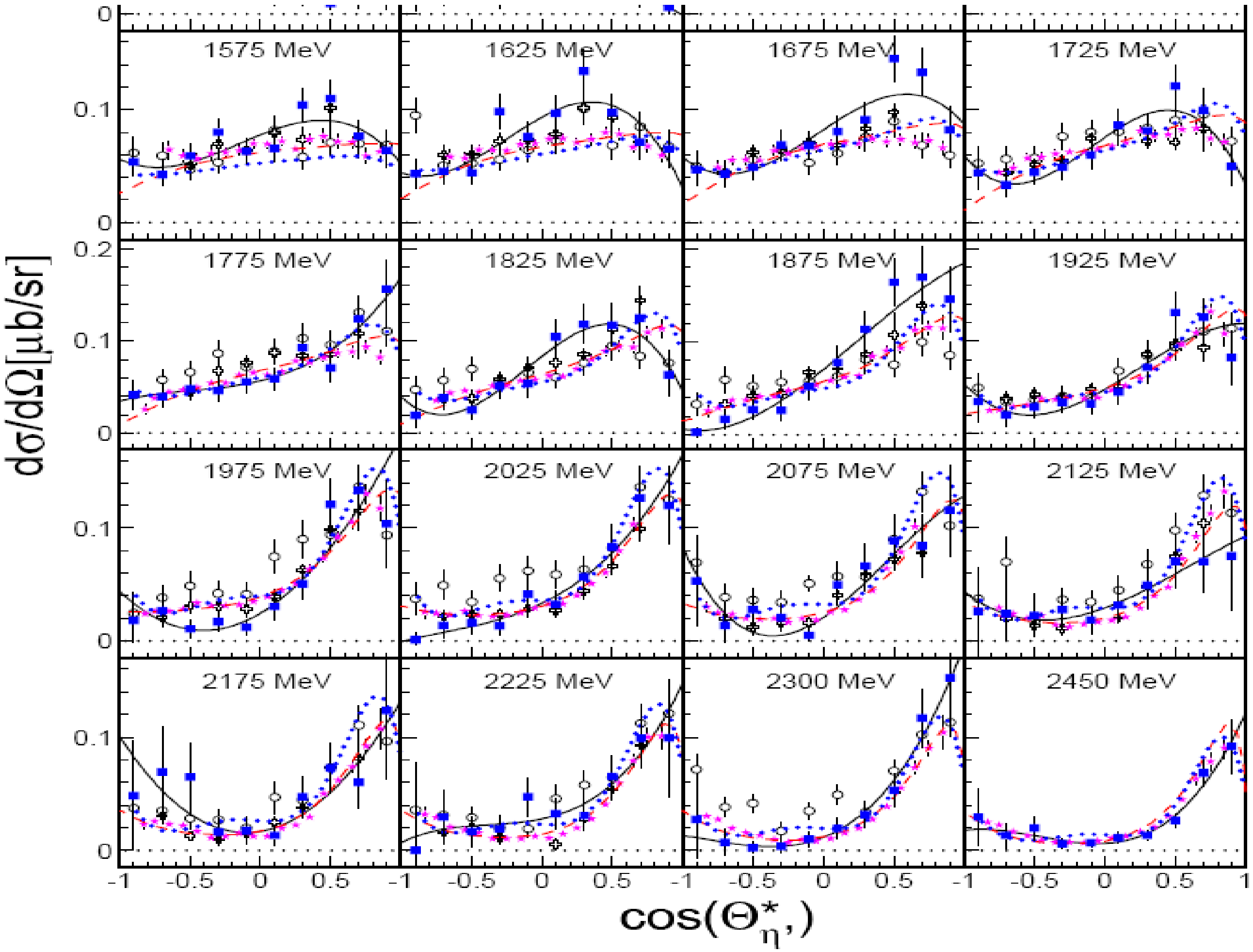

Fig. 9. Comparison of quasi-free η' production off the bound proton ((blue) squares) to the free proton data: (black) open circles [18], (black) open crosses: [31], (magenta) stars: [19]. The numbers given in the figure indicate the bin centers in incident photon energy (note: first two bins below free nucleon production threshold). Note: results from [31,19] partly not exactly for the same energy bins as present results. Closest bins or average of overlapping bins chosen. All uncertainties only statistical. Lines: Solid (black): Legendre fits to data present data, dashed (red): solution (I) NH model, dotted (blue): η'-MAID.

CBELSA/TAPS Results

γn→η'n

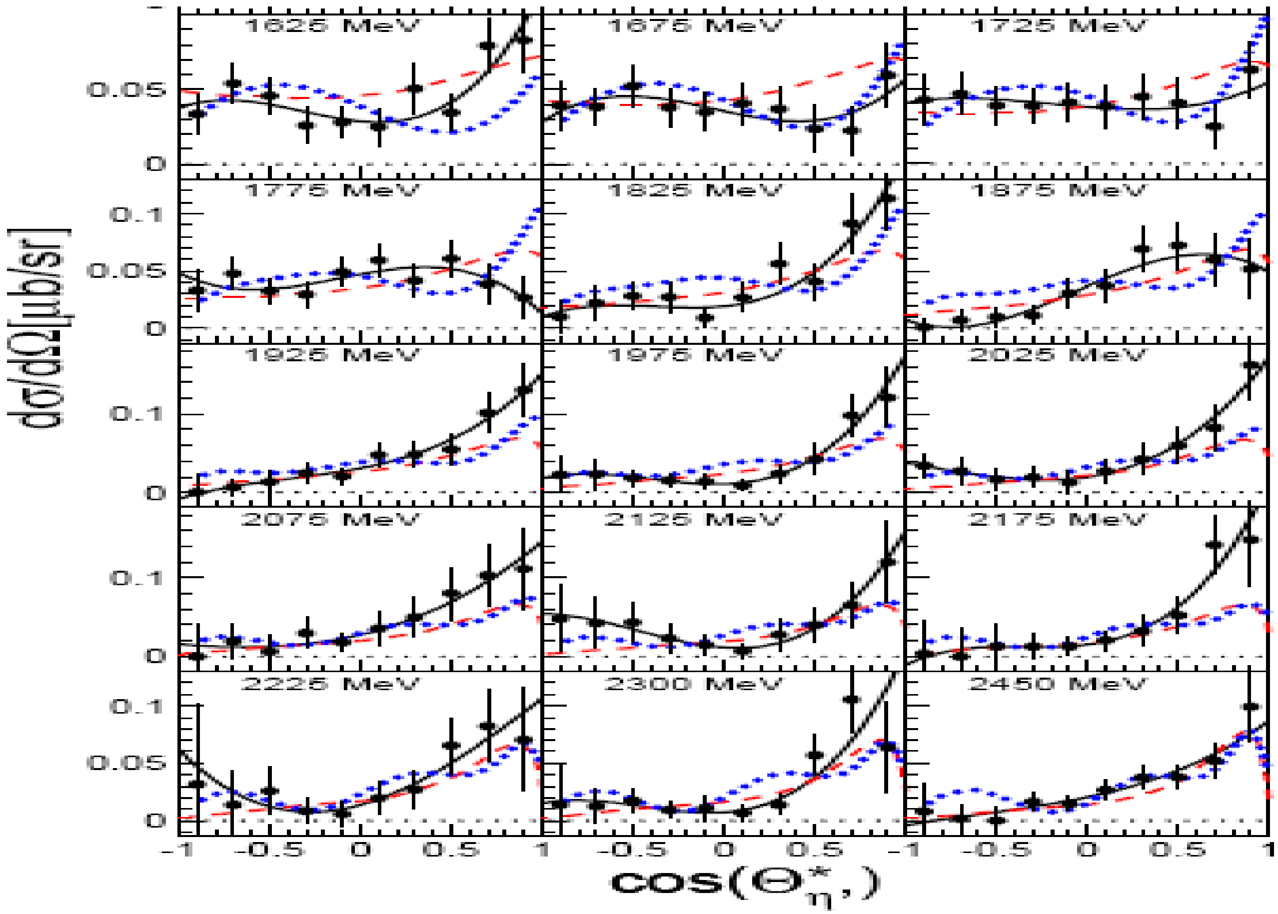

Fig. 12. Angular distributions for the quasi-free $\gamma n \to n\eta'$ reaction. Only statistical uncertainties. Solid (black) lines: Legendre fit to data. Dashed (red) lines: solution (I) of NH model, dotted (blue) lines: η'-MAID model.

II. Our analysis of the γp→η′p and γn→η′n in the chiral quark model

Based on our previous work:
Xian-Hui Zhong, Qiang Zhao,
Phys.Rev. C84 (2011) 045207

Chiral quark model

Zhenping Li, J. Phys. G: Nucl. Part. Phys. 23 ,1127 (1997);
Qiang Zhao, PRC.63.035205(2001)

Reggeized model

Wen-Tai Chiang and Shin Nan Yang et al,
PhysRevC.68.045202 (2003)

meson exchange model

K. Nakayama and H. Haberzettl, PRC.69.065212 (2004);
PRC73, 045211 (2006).
A. Sibirtsev et al, arXiv:nucl-th/0303044

Some other models …

Differential cross sections of γp→η'p

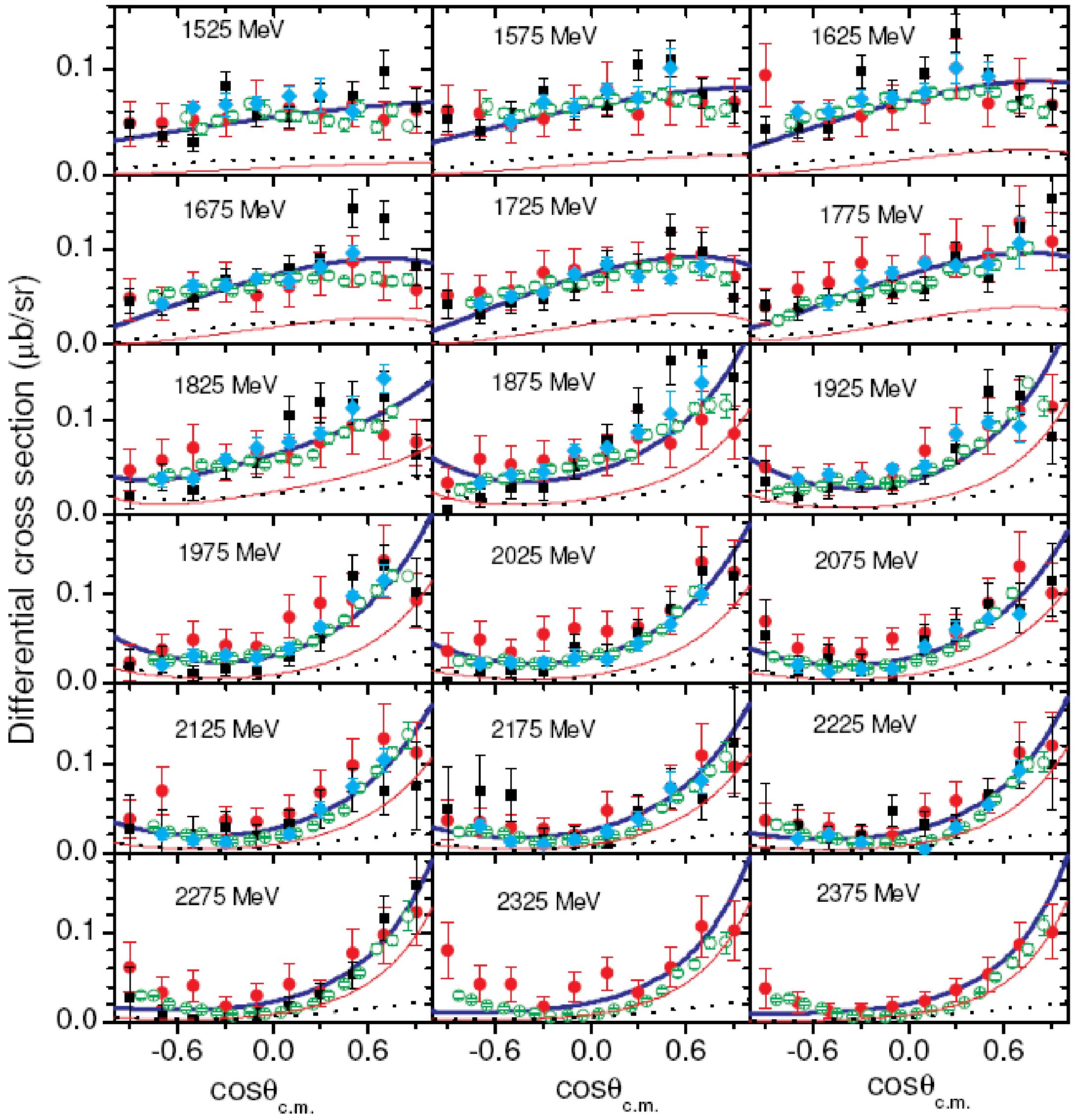

The exp. data can be described within the framework of chiral quark model.

Total cross sections of $\gamma p \rightarrow \eta' p$

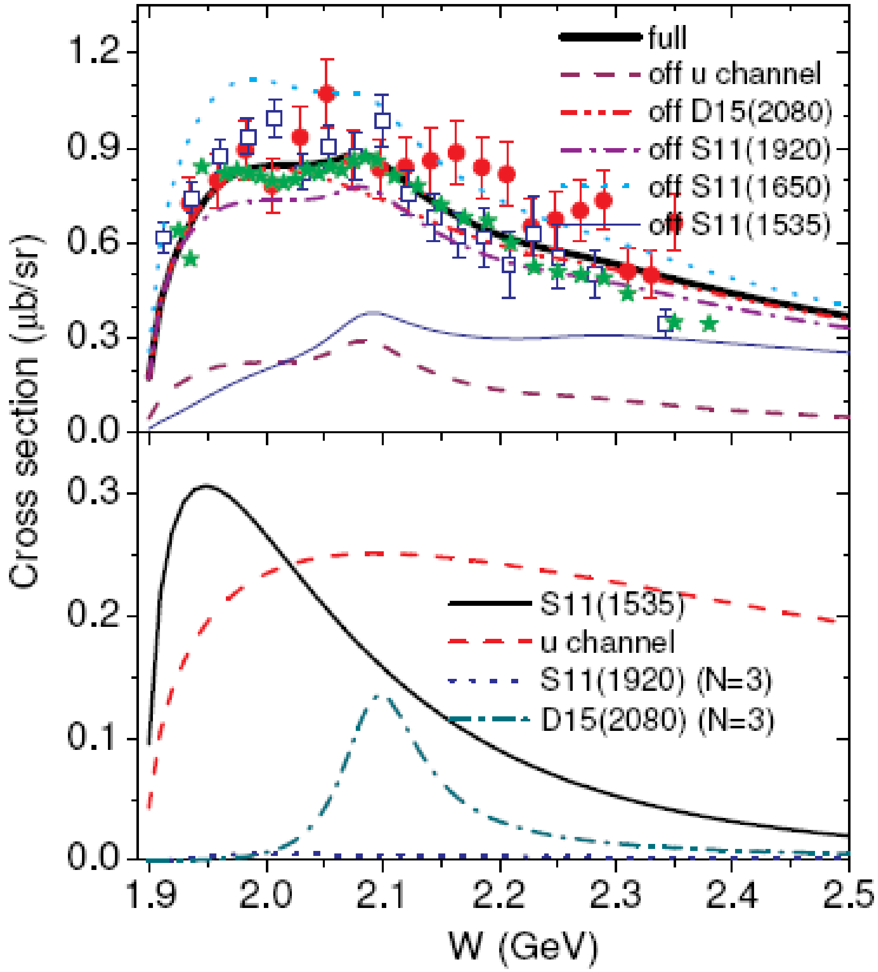

The contributions of D_{15}(2080) (n=3) can explain the bump structure around 2.1 GeV.

The role of D_{15}(2080) in the differential cross sections

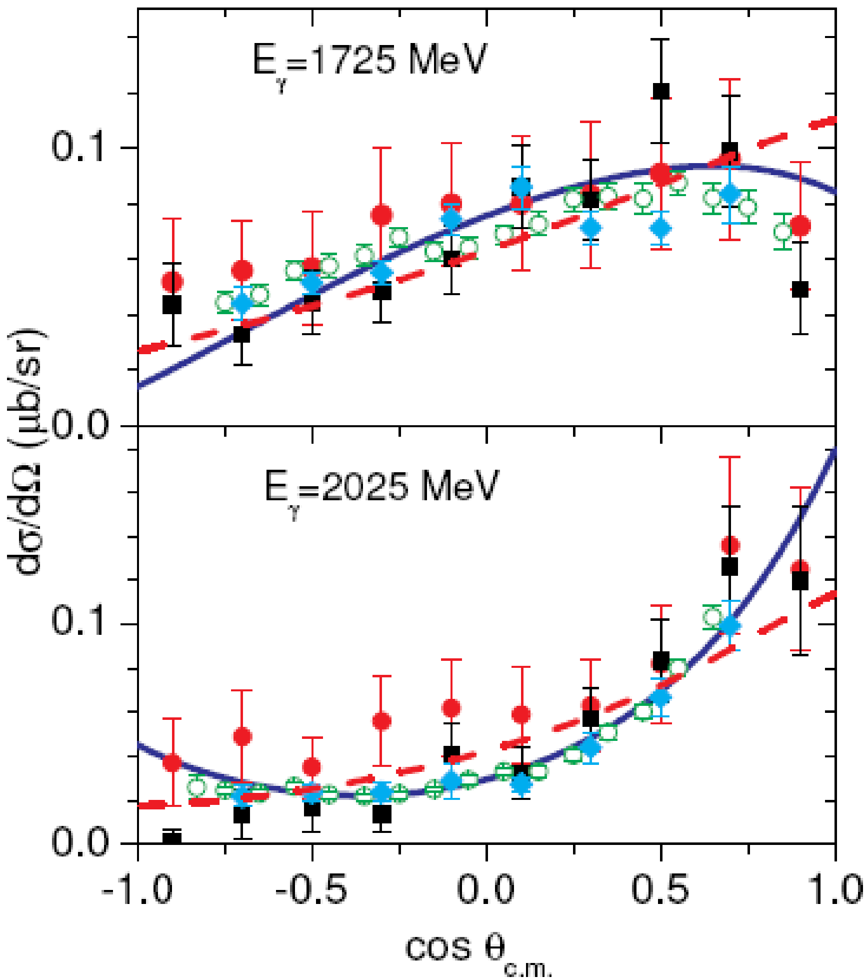

Switching off D_{15}(2080), the bowl shape of the differential cross sections are less obvious. The sudden change of the shape around 1.9 GeV is due to the contributions of D_{15}(2080).

Further evidence of D_{15}(2080) in the exciting function

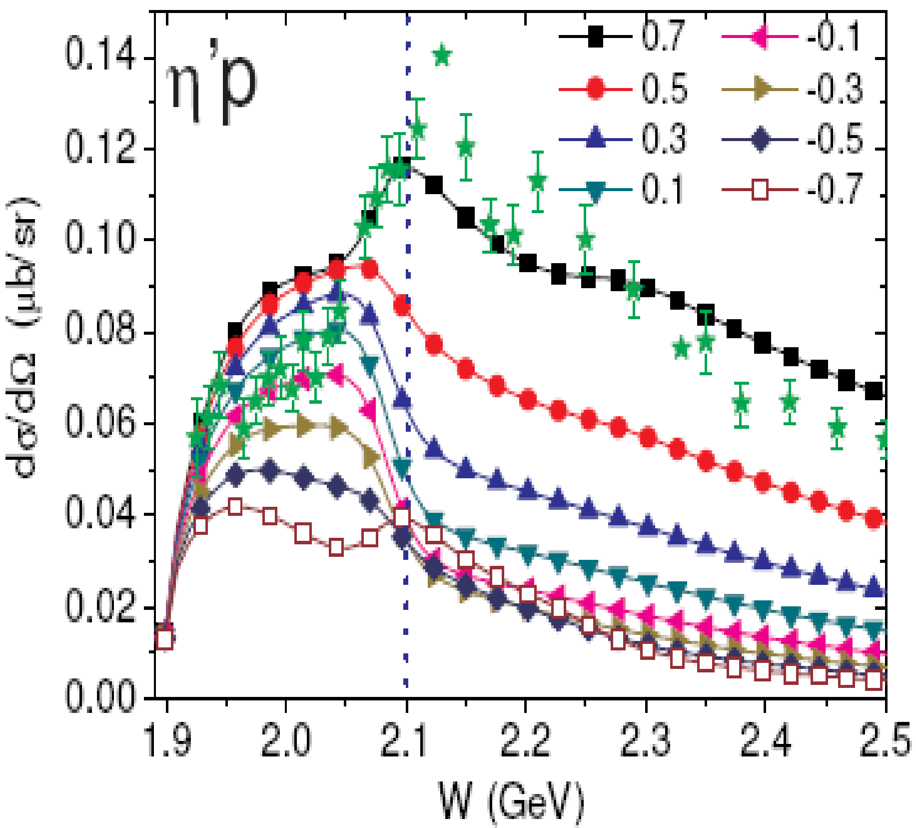

In the forward angle region, there is an obvious peak in the cross sections. This peak is due to the contributions of D_{15}(2080).

The predicted beam asymmetry

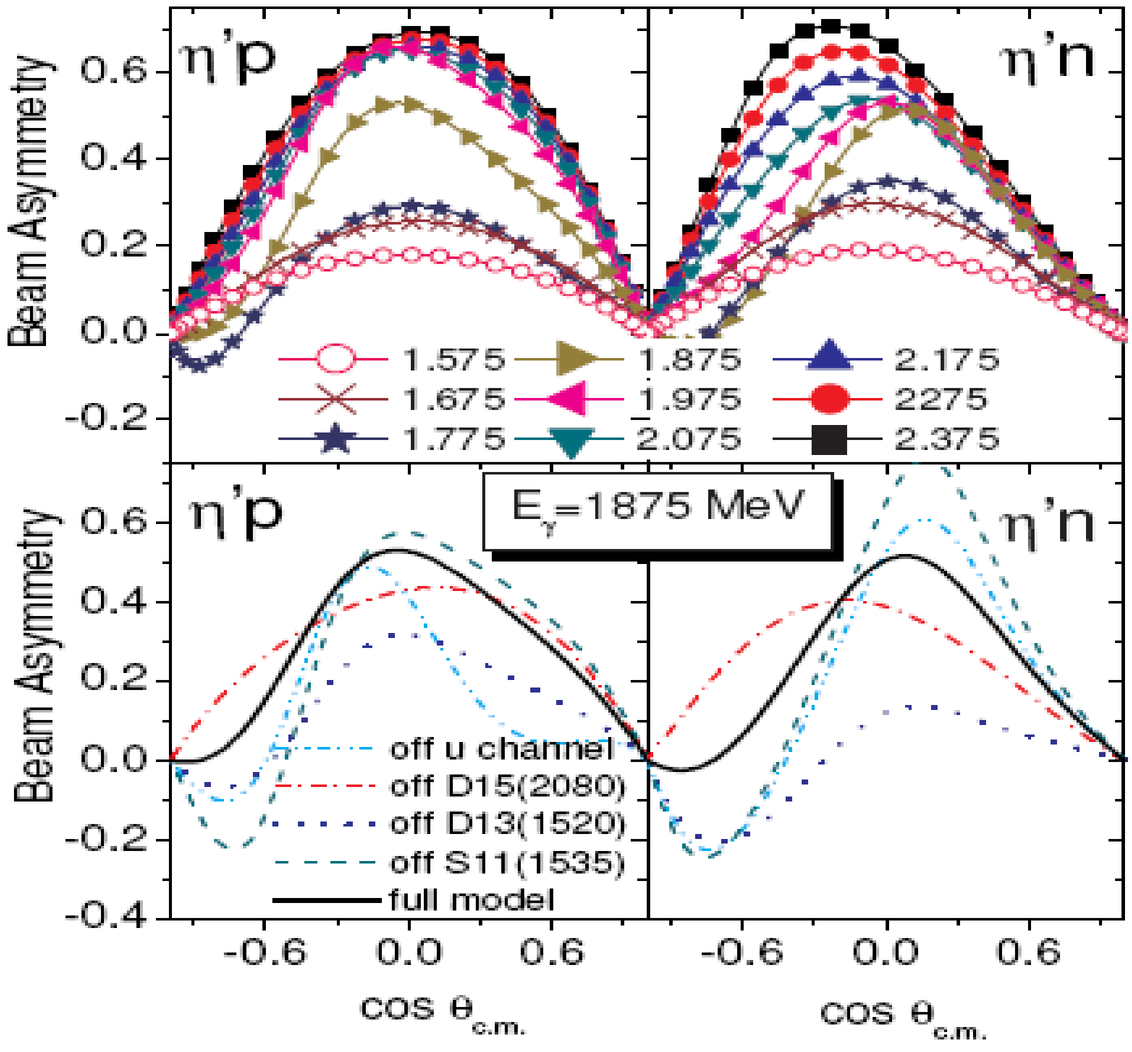

Differential cross sections of γn→η’n

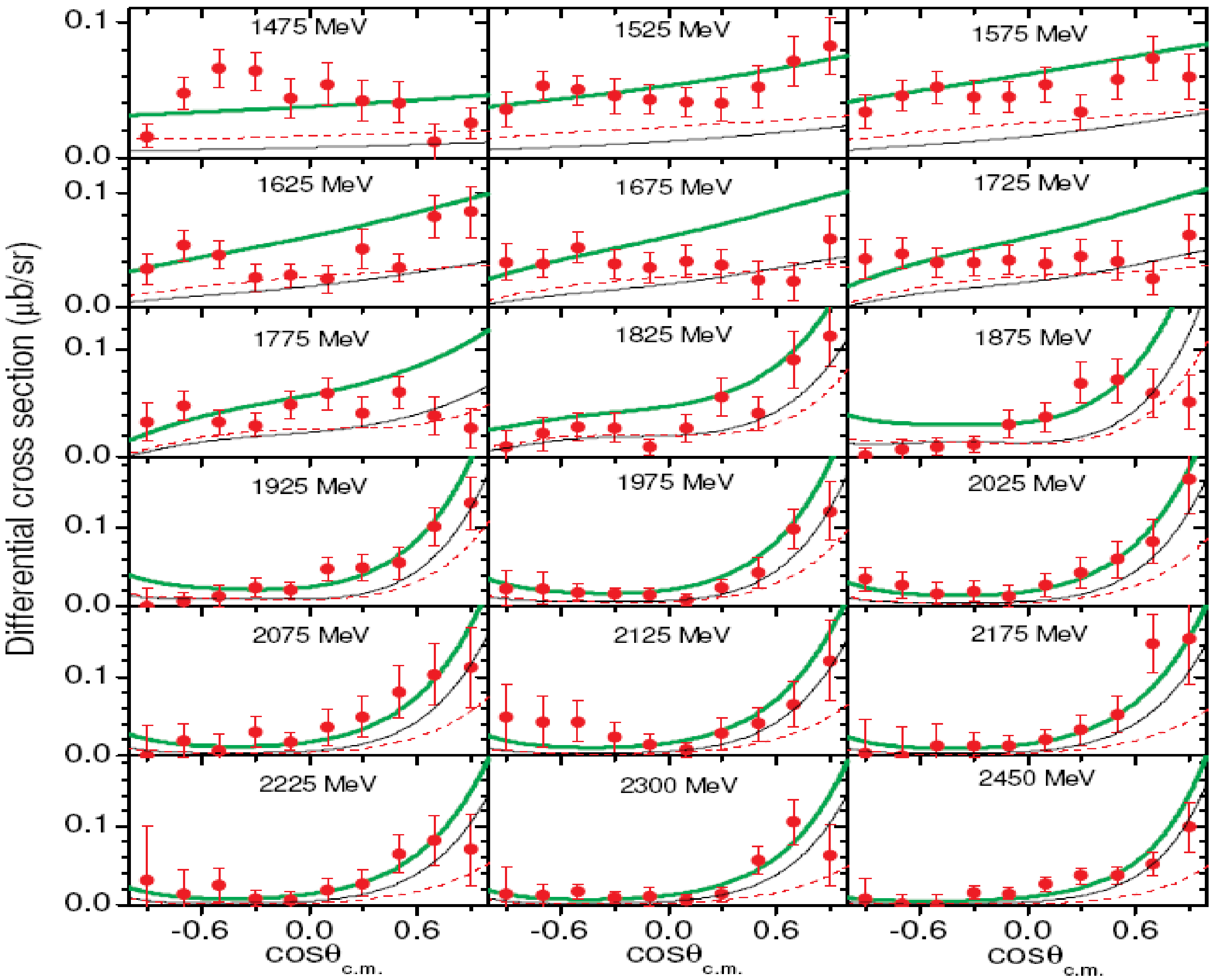

Total cross section for $\gamma n \rightarrow \eta' n$

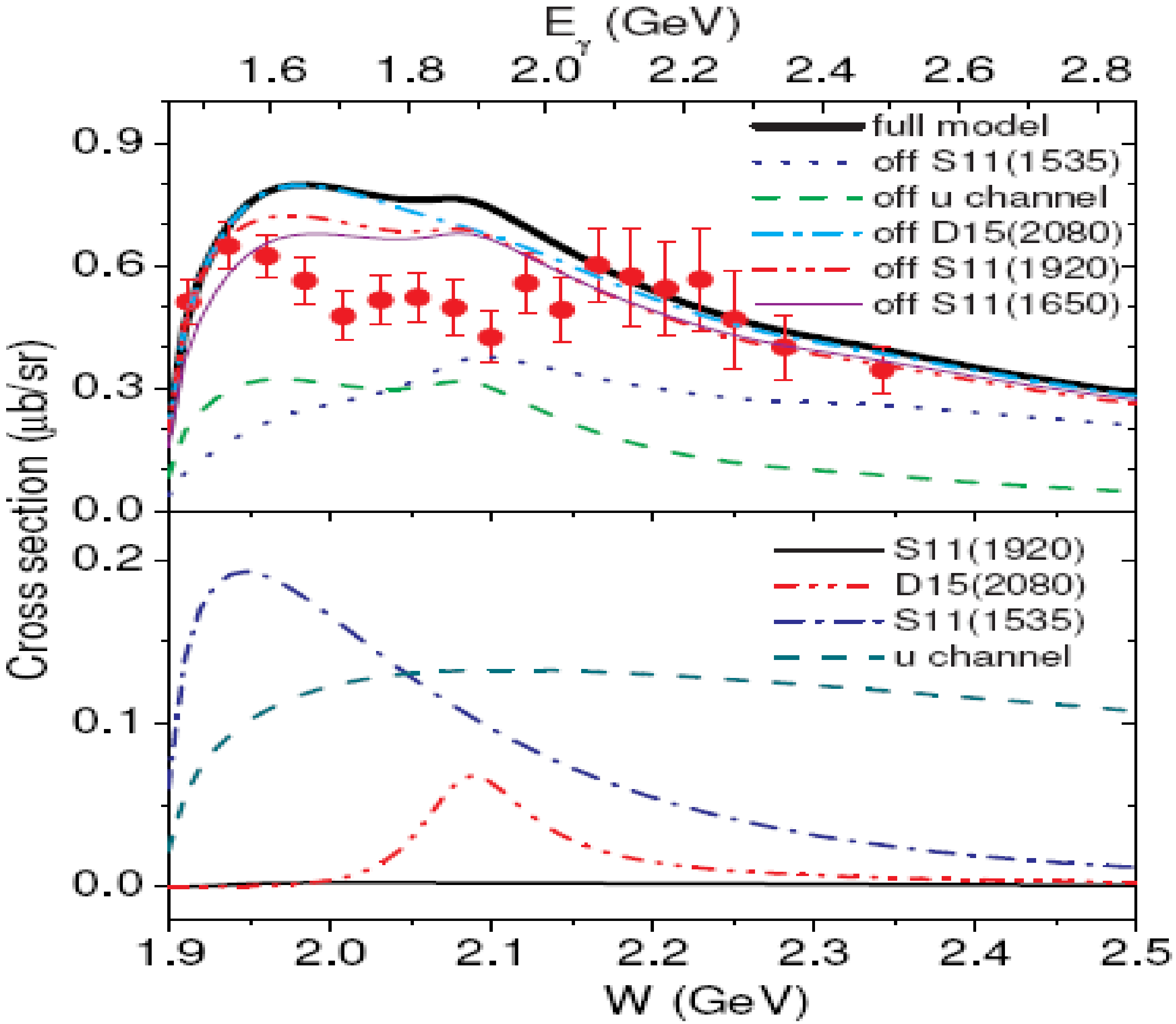

Total cross section for γd→η'np

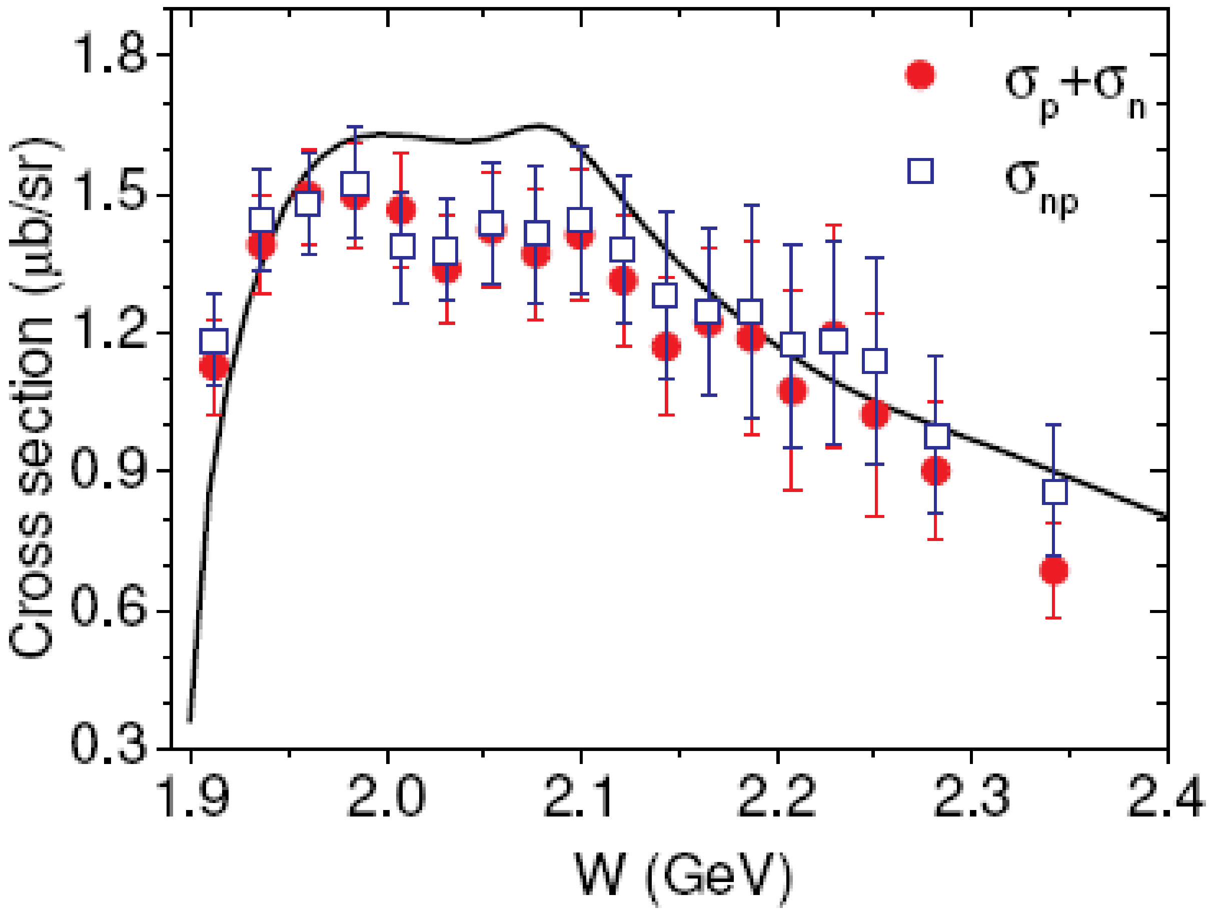

The predicted exciting function $\gamma n \rightarrow \eta' n$

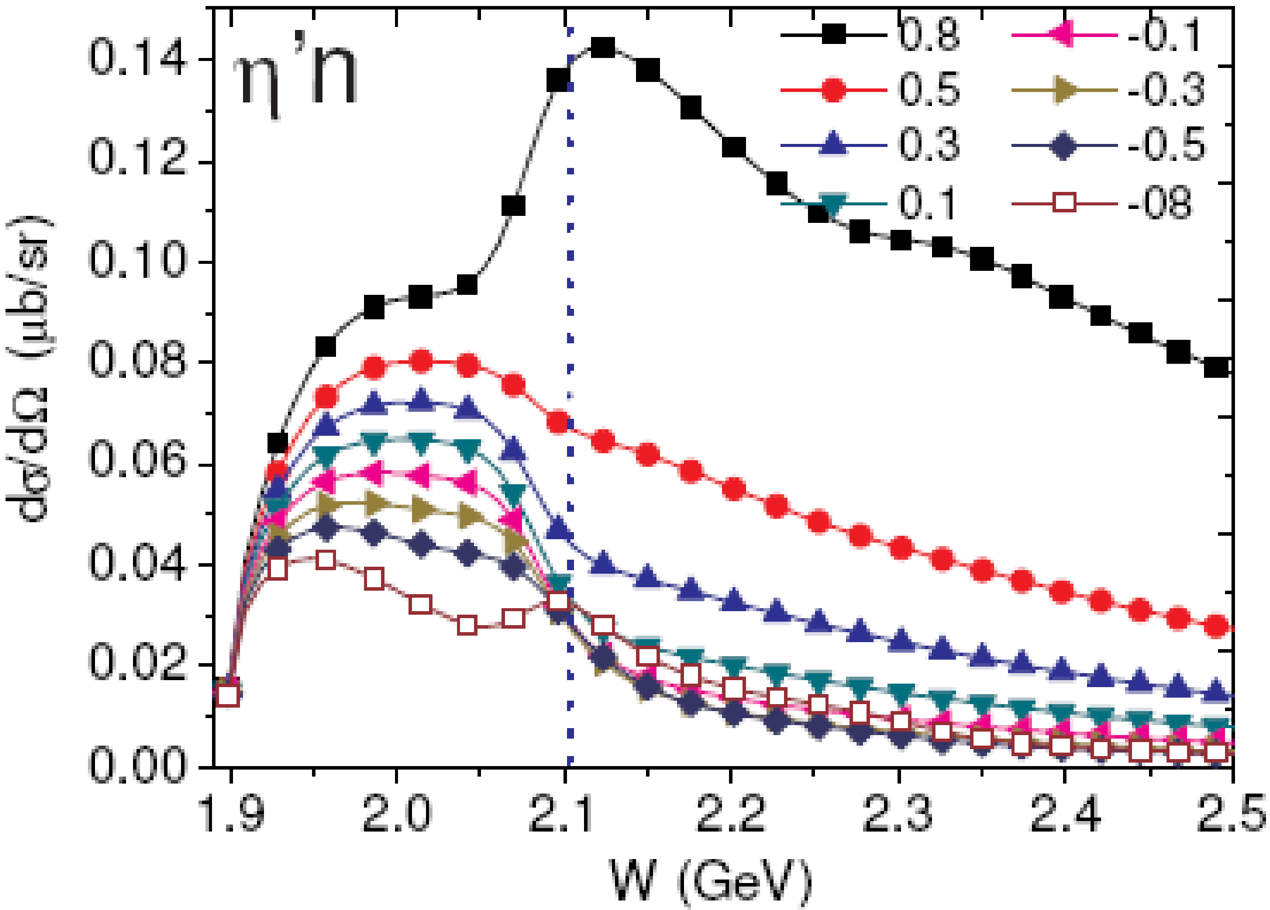

Why does D_{15} play a dominant role in the n=3 shell resonances, rather than D_{13}?

The resonance amplitudes

$$\mathcal{M}_R^s = \frac{2M_R}{s - M_R^2 + i\,M_R\Gamma_R}\mathcal{O}_R e^{-(\mathbf{k}^2+\mathbf{q}^2)/6\alpha^2}, \tag{1}$$

CGLN form

$$\mathcal{O}_R = i f_1^R \sigma\cdot\epsilon + f_2^R \frac{(\sigma\cdot\mathbf{q})\sigma\cdot(\mathbf{k}\times\epsilon)}{|\mathbf{q}||\mathbf{k}|} + i f_3^R \frac{(\sigma\cdot\mathbf{k})(\mathbf{q}\cdot\epsilon)}{|\mathbf{q}||\mathbf{k}|} + i f_4^R \frac{(\sigma\cdot\mathbf{q})(\mathbf{q}\cdot\epsilon)}{|\mathbf{q}|^2}, \tag{2}$$

CGLN amplitudes for n=3 shell resonances

	f_1^R	f_2^R
S_{11}	$-\frac{i}{36}\frac{\omega_m\omega_\gamma}{\mu_q}(g_2+\frac{k}{2m_q}g_1)x^2 + \frac{i}{60}(g_1\frac{k}{m_q}+2g_2)Ax^3$	0
D_{13}	$\frac{i}{90}\frac{\omega_m\omega_\gamma}{\mu_q}(g_2+\frac{k}{2m_q}g_1)x^2 - \frac{i}{60}(g_1\frac{k}{m_q}+2g_2)Ax^3$	$\frac{i}{180}\frac{\omega_m\omega_\gamma^2}{\mu_q m_q}g_1x^2P_2'(z) - \frac{i}{105}\frac{k}{m_q}(g_1+g_3/2)Ax^3P_2'(z)$
D_{15}	$\{-\frac{i}{90}\frac{\omega_m\omega_\gamma}{\mu_q}(g_2+\frac{k}{2m_q}g_1)x^2 + \frac{i}{105}[(g_1-\frac{1}{2}g_3)\frac{k}{m_q}+g_2]Ax^3\}P_3'(z)$	$-\frac{i}{180}\frac{\omega_m\omega_\gamma^2}{\mu_q m_q}g_1x^2P_2'(z) + \frac{i}{420}\frac{k}{m_q}(5g_1-3g_3)Ax^3P_2'(z)$
G_{17}	$\frac{-i}{1890}[(4g_1+5g_3)\frac{k}{m_q} + 18g_2]Ax^3P_3'(z)$	$\frac{-i}{210}(8g_2-g_1\frac{k}{m_q})Ax^3P_4'(z)$
G_{19}	$i\frac{2k}{945m_q}(g_1-g_3)Ax^3P_5'(z)$	$i\frac{k}{378m_q}(g_1-g_3)Ax^3P_4'(z)$

CGLN amplitudes for n=3 shell resonances

	f_3^R	f_4^R
S_{11}	0	0
D_{13}	0	$-\frac{i}{90}\frac{\omega_m\omega_\gamma}{\mu_q m_q}g_2x^2P_2''(z)+\frac{i}{420}Ax^3[14g_2-(g_1-g_3)\frac{k}{m_q}]P_2''(z)$
D_{15}	$-\frac{i}{90}\frac{\omega_m\omega_\gamma}{\mu_q}g_2x^2P_3''(z)+\frac{i}{420}[4g_2-(g_1-g_3)\frac{k}{m_q}]Ax^3P_3''(z)$	$\frac{i}{90}\frac{\omega_m\omega_\gamma}{\mu_q}g_2x^2P_2''(z)-\frac{i}{420}[4g_2-(g_1-g_3)\frac{k}{m_q}]Ax^3P_2''(z)$
G_{17}	$\frac{i}{1890}[(g_1-g_3)\frac{k}{m_q}-18g_2]Ax^3P_3''(z)$	$\frac{-i}{1890}[(g_1-g_3)\frac{k}{m_q}-18g_2]Ax^3P_4''(z)$
G_{19}	$-i\frac{k}{1890m_q}(g_1-g_3)Ax^3P_5''(z)$	$i\frac{k}{1890m_q}(g_1-g_3)Ax^3P_4''(z)$

$$\left| f_1^R[D_{15}(n=3)] \right| > \left| f_1^R[D_{13}(n=3)] \right| P_3'(\cos\theta), \quad (8)$$

$$\left| f_i^R[D_{15}(n=3)] \right| > \left| f_i^R[D_{13}(n=3)] \right| \quad (i=2,3,4), \quad (9)$$

$$\left| f_1^R[D_{15}(n=3)] \right|_{\cos\theta \simeq \pm 1} > 6 \left| f_1^R[D_{13}(n=3)] \right|. \quad (10)$$

At very forward and backward angles, the magnitude for D_{15} is about an order larger than that of D_{13}!

At very forward and backward angle regions, the angle distributions are sensitive to the D_{15} partial wave.

Evidence of $D_{15}(2080)$ might exist in the other processes :

$\gamma p \to \eta p$

$\gamma p \to K^+ \Lambda(1520)$

$J/\Psi \to N\ \text{anti}N\ \pi$……

CB-ELSA Result

$\gamma p \rightarrow \eta p$

PRL 94, 012004 (2005),

Eur. Phys. J. A 25, 427-439 (2005)

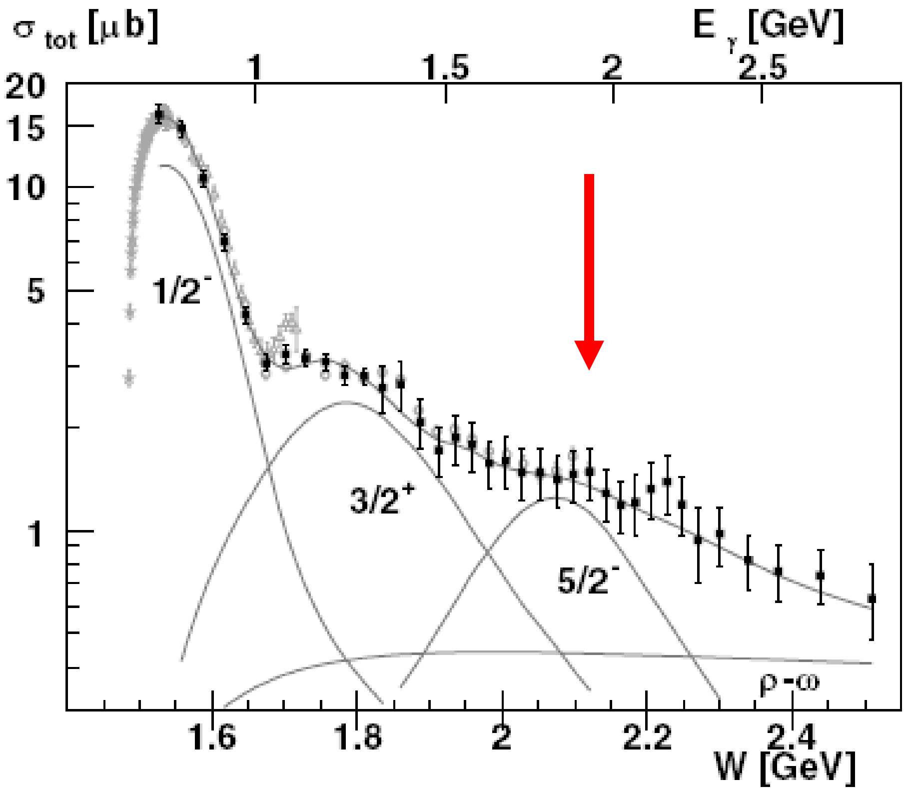

E. Klempt et al fit the data, they suggested that $D_{15}(2070)$ was required in the analysis of the data of the $\gamma p \rightarrow \eta p$ differential cross sections!

Jun He et al, PR C 78, 035204 (2008)

Jun He et al also found some effects from a D_{15}(2090) by analyzing the γp→ηp data with the chiral quark model.

TABLE IV. The χ^2s shown are the values after turning off the corresponding (known) resonance contribution within the model B, for which $\chi^2 = 2.31$.

Removed N^*	$S_{11}(1535)$	$S_{11}(1650)$	$P_{11}(1440)$	$P_{11}(1710)$	$P_{13}(1720)$	$P_{13}(1900)$
χ^2	162	11.9	2.29	2.39	4.15	2.35
Removed N^*	$D_{13}(1520)$	$D_{13}(1700)$	$D_{15}(1675)$	$F_{15}(1680)$	$F_{15}(2000)$	$F_{17}(1990)$
χ^2	9.83	2.29	2.24	4.82	2.33	2.31
Removed N^*	HM N^*	New S_{11}	New D_{13}	New D_{15}		
χ^2	2.50	12.69	2.63	3.88		

BESII Result

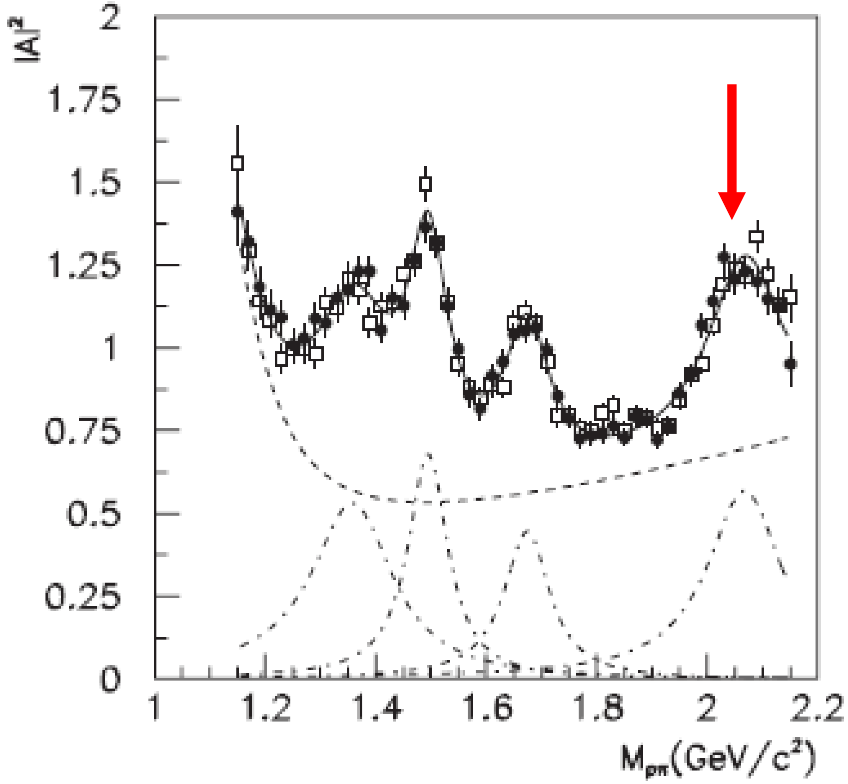

TABLE I. The fitted masses and widths for the four N^* peaks shown in Fig. 6.

Mass (MeV/c^2)	Width (MeV/c^2)
$1358 \pm 6 \pm 16$	$179 \pm 26 \pm 50$
$1495 \pm 2 \pm 3$	$87 \pm 7 \pm 10$
$1674 \pm 3 \pm 4$	$100 \pm 9 \pm 15$
$2068 \pm 3^{+15}_{-40}$	$165 \pm 14 \pm 40$

J/Ψ→N antiN π

PRL 97, 062001 (2006)

BESII observed a structure around 2060 MeV in the πN invariant mass spectrum, which may be one or more of the long-sought missing *N* star resonance.

LEPS Results

$\gamma p \to K^+\Lambda(1520)$

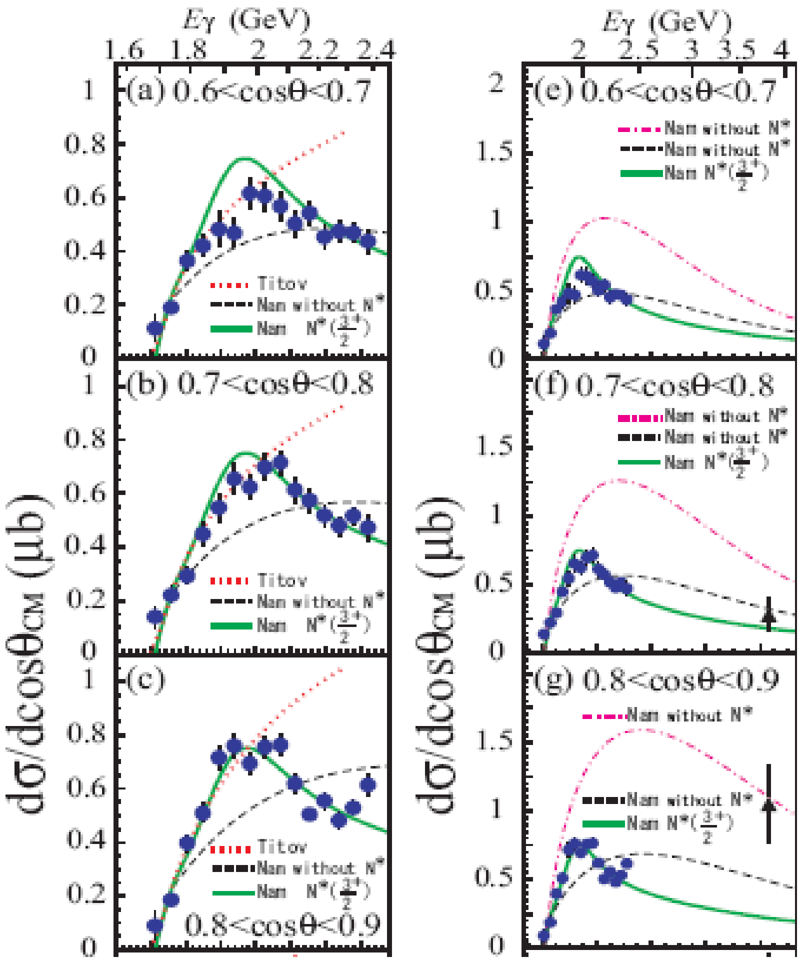

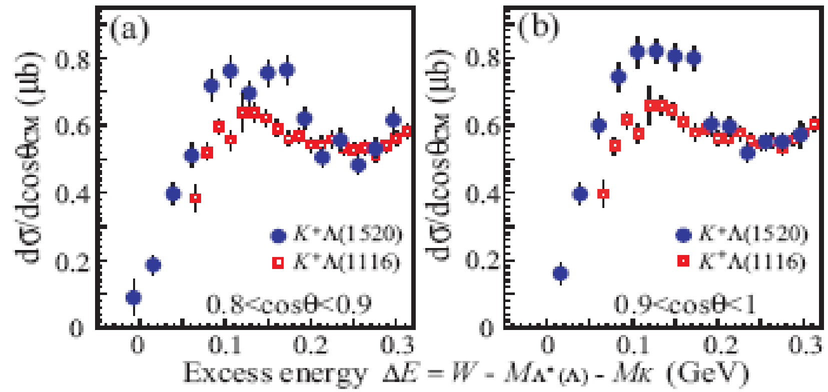

LEPS observed a structure around 2.11 GeV in the cross sections.

Phys.Rev.Lett.104:172001,2010

The bump is not well reproduced by theoretical calculations introducing a nucleon resonance with $J^P \leq 3/2$, This result suggests that the bump might be produced by a nucleon resonance possibly with $J^P \geq 5/2$ or by a new reaction process, for example an interference effect with the photoproduction having a similar bump structure in the cross sections.
[Phys.Rev.Lett.104:172001,2010]

Recently, Ju-Jun Xie and J. Nieves analyzed the data, they claimed that the inclusion of the nucleon resonance $D_{13}(2080)$ leads to a fairly good description of the new LEPS differential cross section data.
[Phys.Rev.C82:045205,2010]

III. Summary

- **The exp. data for eta' photoproduction can be well described in the chiral quark model.**

- **There is strong evidence of D_{15}(2080) in the $\gamma p \rightarrow \eta' p$.**

Thanks !